

Introducing Interval Neural Networks for Uncertainty-Aware System Identification

Mehmet Ali Ferah

*Artificial Intelligence and Intelligent Lab.
Istanbul Technical University
Istanbul, Türkiye
ferah23@itu.edu.tr*

Tufan Kumbasar

*Artificial Intelligence and Intelligent Lab.
Istanbul Technical University
Istanbul, Türkiye
kumbasart@itu.edu.tr*

Abstract—System Identification (SysID) is crucial for modeling and understanding dynamical systems using experimental data. While traditional SysID methods emphasize linear models, their inability to fully capture nonlinear dynamics has driven the adoption of Deep Learning (DL) as a more powerful alternative. However, the lack of uncertainty quantification (UQ) in DL-based models poses challenges for reliability and safety, highlighting the necessity of incorporating UQ. This paper introduces a systematic framework for constructing and learning Interval Neural Networks (INNs) to perform UQ in SysID tasks. INNs are derived by transforming the learnable parameters (LPs) of pre-trained neural networks into interval-valued LPs without relying on probabilistic assumptions. By employing interval arithmetic throughout the network, INNs can generate Prediction Intervals (PIs) that capture target coverage effectively. We extend Long Short-Term Memory (LSTM) and Neural Ordinary Differential Equations (Neural ODEs) into Interval LSTM (ILSTM) and Interval NODE (INODE) architectures, providing the mathematical foundations for their application in SysID. To train INNs, we propose a DL framework that integrates a UQ loss function and parameterization tricks to handle constraints arising from interval LPs. We introduce novel concept “elasticity” for underlying uncertainty causes and validate ILSTM and INODE in SysID experiments, demonstrating their effectiveness.

Index Terms—interval neural networks, system identification, uncertainty quantification, prediction intervals.

I. INTRODUCTION

System identification (SysID) is the process of modeling dynamic systems based on data, where the system’s future behavior depends on its historical dynamics [1]. Traditional SysID methods are well-developed but emphasize linear modeling [2], [3], making them potentially inefficient for representing the nonlinear relationships observed in real-world systems. Integrating Deep learning (DL) into SysID has emerged as a powerful method, as DL can effectively capture complex mappings by modeling high-dimensional and nonlinear dynamics [4], [5]. Long Short-Term Memory (LSTM) [6] and Neural Ordinary Differential Equations (NODEs) [7] networks are among the most widely used Neural Network (NN) architectures in SysID [8], [9]. Both have strengths that complement each other: LSTMs excel at discrete updates, while NODEs can also handle continuous dynamics effectively [10].

The primary challenge with NNs is that their point predictions can be unreliable. To address this, Uncertainty Quantification (UQ) becomes crucial, as it allows for a more comprehensive evaluation of prediction reliability by quantifying the uncertainty associated with the model’s outputs [11], [12], [13], [14]. Instead of point predictions, UQ introduces Prediction Intervals (PIs), offering a range where the true outcome likely falls [15], [16]. Popular methods for UQ typically model uncertainty in Learnable Parameters (LPs) by assuming they follow prior distributions [17]. Predefined distributions constrain model flexibility, potentially limiting generalization. Interval Neural Network (INN) provide an alternative approach for PIs that doesn’t rely on probabilistic assumptions [18]. Recent studies have explored the application of INNs across a wide range of fields [19], [20], [21], [22].

This paper presents a systematic method for constructing and learning INNs with the capability to perform UQ for SysID tasks. We propose constructing the INN by transforming the LPs of a pre-trained NN into interval LPs, without relying on probabilistic assumptions. Thus, by representing uncertainty via interval LPs and incorporating interval arithmetic operations throughout the layers, INNs can effectively capture the uncertainty. This approach enables the generation of Prediction Intervals (PIs), providing a measure of uncertainty in the predictions. We provide all the mathematical foundations on how to extend LSTM and NODE into Interval LSTM (ILSTM) and Interval NODE (INODE). To train the ILSTM and INODE that ensure PIs satisfy the desired coverage, we propose a DL framework that incorporates a UQ loss and parameterization tricks to eliminate the constraint arising from the interval LPs. The DL framework is designed to effectively transform LPs of a pre-trained NN into interval LPs while minimizing the width of the PIs, thereby balancing the trade-off between coverage accuracy and interval precision. To evaluate the UQ performances of ILSTM and INODE, we conduct a series of SysID experiments. The results show that both methods are effective in capturing uncertainty, with INODE demonstrating better performance in terms of coverage. To understand the underlying reasons, we introduce the concept of “elasticity,” which provides a fresh perspective for analyzing uncertainty in LPs. The results of this study demonstrate that the proposed INNs effectively tackle SysID tasks while enabling UQ.

II. PRELIMINARIES ON INTERVAL ARITHMETIC

Definition 1. For $x \in \mathbb{R}$, a *crisp number* a is a single, deterministic and finite value such that:

$$x = a, \quad a \in \mathbb{R}$$

Definition 2. Let $\underline{a}, \bar{a} \in \mathbb{R}$ and $\underline{a} \leq \bar{a}$. An *interval number* $\tilde{a} = [\underline{a}, \bar{a}]$ is defined as the closed subset of crisp numbers, defined in Definition 1, given by [23]:

$$\tilde{a} = [\underline{a}, \bar{a}] = \{x \in \mathbb{R} \mid \underline{a} \leq x \leq \bar{a}\}.$$

Special Case: When $\underline{a} = \bar{a}$, the interval $[\underline{a}, \bar{a}]$ collapses to a single point a , representing a crisp number [23].

Given interval numbers $[\underline{a}, \bar{a}]$ and $[\underline{b}, \bar{b}]$, the following operations are defined for interval arithmetic [23]:

- Addition: $[\underline{a}, \bar{a}] + [\underline{b}, \bar{b}] = [\underline{a} + \underline{b}, \bar{a} + \bar{b}]$
- Subtraction: $[\underline{a}, \bar{a}] - [\underline{b}, \bar{b}] = [\underline{a} - \bar{b}, \bar{a} - \underline{b}]$
- Multiplication: $[\underline{a}, \bar{a}][\underline{b}, \bar{b}] = [\min(S), \max(S)]$, where $S = \{\underline{a} \cdot \underline{b}, \underline{a} \cdot \bar{b}, \bar{a} \cdot \underline{b}, \bar{a} \cdot \bar{b}\}$.

We define an interval matrix with $\underline{A}, \bar{A} \in \mathbb{R}^{m \times n}$, as follows:

$$[\underline{A}, \bar{A}] = \{X \in \mathbb{R}^{m \times n} \mid \underline{A} \leq X \leq \bar{A}\} \quad (1)$$

Basic matrix operations, such as addition, subtraction, and multiplication, can be easily extended to interval matrices.

- Addition and Subtraction: Let $[\underline{A}, \bar{A}]$ and $[\underline{B}, \bar{B}]$ be as defined in (1). The interval operations are defined as:

$$[\underline{A}, \bar{A}] + [\underline{B}, \bar{B}] = [\underline{A} + \underline{B}, \bar{A} + \bar{B}] \quad (2)$$

$$[\underline{A}, \bar{A}] - [\underline{B}, \bar{B}] = [\underline{A} - \bar{B}, \bar{A} - \underline{B}] \quad (3)$$

- Multiplication: Let $[\underline{A}, \bar{A}]$ and $[\underline{B}, \bar{B}]$ as in (1) but with $\underline{A}, \bar{A} \in \mathbb{R}^{m \times p}$ and $\underline{B}, \bar{B} \in \mathbb{R}^{p \times n}$. It is defined as:

$$[\underline{C}, \bar{C}] = [\underline{A}, \bar{A}][\underline{B}, \bar{B}] \quad (4)$$

Here, the interval dot product is required. Let $[\underline{u}, \bar{u}]$ and $[\underline{v}, \bar{v}]$ be interval vectors with $\underline{u}, \bar{u}, \underline{v}, \bar{v} \in \mathbb{R}^n$.

$$[\underline{u}, \bar{u}] \cdot [\underline{v}, \bar{v}] = [\min(S1, S2), \max(S1, S2)], \quad (5)$$

where

$$\begin{aligned} S1 &= \sum_{i=1}^n [\underline{u}(i)\bar{u}(i)][\underline{v}(i), \bar{v}(i)] \\ S2 &= \sum_{i=1}^n [\underline{u}(i)\bar{u}(i)][\underline{v}(i), \bar{v}(i)]. \end{aligned} \quad (6)$$

III. LEARNING NNS FOR SYSID

Here, we briefly outline how the NNs are defined and learned for SysID problems. We assume having a dataset, $\{(u(k), \hat{y}(k))\}_{k=1}^K$, with an input $u(k)$ and an output $\hat{y}(k)$. To represent the dynamics, we aim to learn an NN as follows:

$$y(k) = g(x(k), \theta) \quad (7)$$

with

$$x(k) = \begin{bmatrix} u(k - n_d), \dots, u(k - n_d - n_x), \\ y(k - 1), \dots, y(k - n_y) \end{bmatrix} \quad (8)$$

where n_x is input lag, n_y is output lag and n_d is dead time.

To train the NN model within a DL framework, we first extract $B = K - N$ trajectories with window length N to define the mini-batches via Algorithm-1. Then, the model is trained with a DL optimizer in mini-batches of size mbs . The optimization problem to minimized is defined as follows:

$$\theta^* = \arg \min_{\theta} \left\{ \frac{1}{BN} \sum_{m=1}^B \sum_{k=1}^N \left(\hat{Y}(m, k) - Y(m, k) \right)^2 \right\} \quad (9)$$

During training and inference, the model operates in simulation mode, with $x(k)$ updated after each prediction.

This paper uses LSTM and NODE networks to represent $g(\cdot)$ in (7). All networks are implemented using feedforward NNs as layers. The remainder of this section provides a brief overview of handled feedforward NNs, LSTMs, and NODEs.

A. Feedforward Neural Networks

An n -layer NN is a function with an input x as follows:

$$y = g(x; \theta) \quad (10)$$

with crisp LPs $\theta = \{\theta_i\}_{i=1}^n$. Here, g is defined as:

$$g(x; \theta) = g_n(g_{n-1}(g_1(x; \theta_1); \dots; \theta_{n-1}); \theta_n) \quad (11)$$

The inference of g_i is defined for $x_i \in \mathbb{R}^m$ as follows:

$$g_i(x_i; \theta_i) = \sigma_i(W_i x_i + b_i) \quad (12)$$

with $\sigma = \{\sigma_i\}_{i=1}^n$ represents the activation functions and $\theta_i = (W_i, b_i)$ consists $W_i \in \mathbb{R}^{p \times m}$ and $b_i \in \mathbb{R}^p$.

B. Long Short Term Memory Network

For a sampled input $x(k)$, an n -layer LSTM is defined :

$$(h(k), c(k)) = g(x(k), h(k-1), c(k-1); \theta) \quad (13)$$

where each layer is characterized by the input gate $i(k)$, forget gate $f(k)$, output gate $o(k)$, hidden state $h(k)$, and cell state $c(k)$ at time step k , which are defined as [8]:

$$\begin{aligned} i_i(k) &= \sigma^{\text{sig}}(W_i^i x_i(k) + U_i^i h_i(k-1) + b_i^i) \\ f_i(k) &= \sigma^{\text{sig}}(W_i^f x_i(k) + U_i^f h_i(k-1) + b_i^f) \\ o_i(k) &= \sigma^{\text{sig}}(W_i^o x_i(k) + U_i^o h_i(k-1) + b_i^o) \\ \tilde{c}_i(k) &= \sigma^{\text{tanh}}(W_i^c x_i(k) + U_i^c h_i(k-1) + b_i^c) \\ c_i(k) &= f_i(k) \odot c_i(k-1) + i_i(k) \odot \tilde{c}_i(k) \\ h_i(k) &= o_i(k) \odot \sigma^{\text{tanh}}(c_i(k)) \end{aligned} \quad (14)$$

with $\theta_i = (W_i^f, U_i^f, b_i^f, W_i^i, U_i^i, b_i^i, W_i^c, U_i^c, b_i^c, W_i^o, U_i^o, b_i^o)$, where i, f, o and c indicate gates. In (14), σ^{sig} and σ^{tanh}

Algorithm 1 Windowing Data

- 1: **Input:** $\{(u(k), \hat{y}(k))\}_{k=1}^K, N$
 - 2: **for** $i = 1$ **to** $K - N$ **do**
 - 3: $\{(U(k, :), \hat{Y}(k, :))\} = \{(u(k : k + N - 1), \hat{y}(k : k + N - 1))\}$
 - 4: **end for**
 - 5: **Output:** U, \hat{Y}
-

are the sigmoid and tanh activation functions, respectively. For point prediction, the final layer is defined as:

$$y(k) = W_n h(k) + b_n \quad (15)$$

C. Neural Ordinary Differential Equations Networks

Given the input $(x(t), t)$, state $h(t)$ at time t , the n -layer NODE is defined as [7]:

$$\frac{dh(t)}{dt} = g(x(t), t; \theta) \quad (16)$$

To obtain $h(T)$ at time T , we solve the following integral:

$$h(T) = h(t_0) + \int_{t_0}^T g(x(t), t; \theta) dt \quad (17)$$

In this study, we apply Euler's method and rewrite (17) as [24]:

$$h(k) = h(k-1) + g(x(k); \theta) \quad (18)$$

which is defined with g_i ($i = 1, \dots, n-1$) as:

$$g_i(x_i(k); \theta_i) = \sigma_i(W_i x_i(k) + b_i) \quad (19)$$

and the final layer $i = n$ with :

$$y(k) = W_n x_n(k) + b_n \quad (20)$$

IV. INTERVAL NNS FOR UQ: STRUCTURE AND INFERENCE

This section presents INNs for SysID, which can generate PIs. We first extend the feedforward NN into its INN counterpart as it is used to define layers of ILSTM and INODE in detail. Then, we define the equations of ILSTM and INODE for PI generation. We base our INN construction approach on a pre-trained NN with LP θ^* .

A. Feedforward Interval Neural Network Construction

A pre-trained NN is transformed into an INN by converting its LP θ^* into an interval-valued set $\tilde{\theta}$ as follows:

$$\tilde{\theta}_i = [\underline{\theta}_i, \bar{\theta}_i] = [\theta_i^* - \underline{\Delta}_i, \theta_i^* + \bar{\Delta}_i] \quad (21)$$

where $\tilde{\Delta} = \{\tilde{\Delta}_1, \dots, \tilde{\Delta}_n\}$ are the LPs of the INN, defined as $\tilde{\Delta}_i = [\underline{\Delta}_i, \bar{\Delta}_i]$. Note that we must ensure $\underline{\theta}_i < \bar{\theta}_i$ as required in Definition-2.

Now, let us define the inference of the INN with $\tilde{\theta}$.

$$\tilde{y} = \tilde{g}(x; \tilde{\theta}) \quad (22)$$

Here, the INN uses the interval arithmetic operations presented in Section II. The interval version of (11) is:

$$\tilde{g}(x; \tilde{\theta}) = g_n(g_{n-1}(g_1(x; \tilde{\theta}_1); \dots; \tilde{\theta}_{n-1}); \tilde{\theta}_n) \quad (23)$$

and more specifically, for layer i , by defining $\tilde{W} = [\underline{W}, \bar{W}]$ and $\tilde{b} = [\underline{b}, \bar{b}]$, the forward pass is as follows:

$$g_i(\tilde{x}_i; \tilde{\theta}_i) = \sigma_i(\tilde{W}_i \tilde{x}_i + \tilde{b}_i) \quad (24)$$

The output of each layer is an interval number, thus the last layer outputs an interval defined as $\tilde{y} = [\underline{y}, \bar{y}]$. Note that, given a crisp input to the first layer, one can use the special condition in Definition 2 and write $[\underline{x}_1, \bar{x}_1] = x$.

B. Inference of Interval LSTM

This section introduces ILSTM based on the INN design. Thus, we extend (14) and (15) by defining $\tilde{\theta}$ as in (21). We obtain:

$$\begin{aligned} \tilde{i}_i(k) &= \sigma^{sig}(\tilde{W}_i^i \tilde{x}_i(k) + \tilde{U}_i^i \tilde{h}_i(k-1) + \tilde{b}_i^i) \\ \tilde{f}_i(k) &= \sigma^{sig}(\tilde{W}_i^f \tilde{x}_i(k) + \tilde{U}_i^f \tilde{h}_i(k-1) + \tilde{b}_i^f) \\ \tilde{o}_i(k) &= \sigma^{sig}(\tilde{W}_i^o \tilde{x}_i(k) + \tilde{U}_i^o \tilde{h}_i(k-1) + \tilde{b}_i^o) \\ \tilde{c}_i(k) &= \sigma^{tanh}(\tilde{W}_i^c \tilde{x}_i(k) + \tilde{U}_i^c \tilde{h}_i(k-1) + \tilde{b}_i^c) \\ \tilde{c}_i(k) &= \tilde{f}_i(k) \odot \tilde{c}_i(k-1) + \tilde{i}_i(k) \odot \tilde{c}_i(k) \\ \tilde{h}_i(k) &= \tilde{o}_i(k) \odot \sigma^{tanh}(\tilde{c}_i(k)) \end{aligned} \quad (25)$$

Then, we can define the overall ILSTM network as:

$$(\tilde{h}(k), \tilde{c}(k)) = \tilde{g}(\tilde{x}(k), \tilde{h}(k-1), \tilde{c}(k-1); \tilde{\theta}) \quad (26)$$

with

$$\tilde{y}(k) = \tilde{W}_n \tilde{h}(k) + \tilde{b}_n. \quad (27)$$

As the aim is to generate a PI around the output of the pre-trained LSTM, we define the input $\tilde{x}(k)$ in the INN by updating its output and states by using the pre-trained LSTM's output and state as follows:

$$[\underline{h}(k-1), \bar{h}(k-1)] = [h(k-1), h(k-1)] \quad (28)$$

$$[\underline{c}(k-1), \bar{c}(k-1)] = [c(k-1), c(k-1)] \quad (29)$$

$$[\underline{y}(k-1), \bar{y}(k-1)] = [y(k-1), y(k-1)] \quad (30)$$

C. Inference of Interval NODE

We construct INODE similar to ILSTM by $\tilde{\theta}$ using (21). The equations of INODE are expressed as follows:

$$\tilde{h}(k+1) = \tilde{h}(k) + \tilde{g}(\tilde{x}(k); \tilde{\theta}) \quad (31)$$

For layers $i = 1, \dots, n-1$, we define:

$$\tilde{h}_i(k+1) = \tilde{h}_i(k) + \sigma_i(\tilde{W}_i \tilde{x}_i(k) + \tilde{b}_i) \quad (32)$$

while for the final layer $i = n$, we define:

$$\tilde{h}_n(k+1) = \tilde{h}_n(k) + (\tilde{W}_n \tilde{x}_n(k) + \tilde{b}_n) \quad (33)$$

As we have done in ILSTM, to generate a PI around the output of the pre-trained NODE, we update at each step INN output with:

$$[\underline{y}(k-1), \bar{y}(k-1)] = [y(k-1), y(k-1)] \quad (34)$$

V. LEARNING INTERVAL NNS FOR UQ

In this section, we present a DL framework to train the presented ILSTM and INODE networks for UQ. To train the INN, $L_{\text{RQR-W}}$ loss is used [25]. The problem to be minimized at every epoch is defined as:

$$\tilde{\Delta}^* = \arg \min_{\tilde{\Delta}} \left\{ \frac{1}{BN} \sum_{m=1}^B \sum_{k=1}^N L_{\text{RQR}} + \lambda L_W \right\} \quad (35)$$

where α is the desired coverage to be captured by the PIs. Here, L_{RQR} is the loss related to coverage and is defined as:

$$L_{\text{RQR}} = \begin{cases} \alpha\kappa & \text{if } \kappa \geq 0 \\ (\alpha - 1)\kappa & \text{if } \kappa < 0 \end{cases} \quad (36)$$

where

$$\kappa = (\hat{Y}(m, k) - \underline{Y}(m, k))(\hat{Y}(m, k) - \bar{Y}(m, k)). \quad (37)$$

The L_W term penalizes the PI width to enforce narrower bounds, weighted by the hyperparameter λ . L_W is defined as:

$$L_W = (\bar{Y}(m, k) - \underline{Y}(m, k))^2 / 2 \quad (38)$$

The training procedure for the INN is outlined in Algorithm-2 * Here, we would like to underline that:

- During the training of the INN, we must ensure that all LPs $\tilde{\Delta}$ result in $\tilde{\theta}$ that satisfy the conditions of interval numbers (i.e. Definition-2). Thus, we must guarantee that $\Delta_i \geq 0$. Yet, enforcing this constraint transforms (35) into a constraint optimization problem. Thus, as all the built-in DL optimizers are unconstrained ones, we perform the following parameterization tricks to eliminate the constraints:

$$\underline{\Delta}_i = \sigma_{\Delta}(\underline{\Delta}'_i), \quad \bar{\Delta}_i = \sigma_{\Delta}(\bar{\Delta}'_i) \quad (39)$$

where $\underline{\Delta}'_i$ and $\bar{\Delta}'_i$ are the new LPs, and $\sigma_{\Delta}(\cdot)$ is a function that ensures outputs remain strictly positive. In this paper, we propose two functions for σ_{Δ} , which are absolute function σ^{abs} and the ReLU function σ^{ReLU} .

- The initialization of $\tilde{\Delta}$ is important as it might increase the training time. Given θ^* , the initialization of $\tilde{\Delta}$ is performed for the hidden layers as follows:

$$\{\tilde{\Delta}_1, \dots, \tilde{\Delta}_{n-1}\} = \{[\theta_1^*, \theta_1^*], \dots, [\theta_{n-1}^*, \theta_{n-1}^*]\} r_h \quad (40)$$

where $r_h \in [0, 1]$ is the hidden layer uncertainty rate. The output layer is initialized with:

$$\tilde{\Delta}_n = [\theta_n^*, \theta_n^*] r_o \quad (41)$$

where $r_o \in [0, 1]$ is the is the output layer uncertainty rate. r_h and r_o are hyperparameters to be determined.

VI. COMPARATIVE PERFORMANCE ANALYSIS

This section provides a comprehensive analysis of the learning performances of INNs on the SysID benchmark datasets: MR Damper [26], Heat Exchanger [27], and Hair Dryer [1]. All experiments were conducted in MATLAB® and repeated with 5 different initial seeds for statistical analysis. The dataset configurations are set as given in Table I.

We present a dual-fold evaluation to analyze the proposed INNs.

- Analyzing the coverage performances of proposed INNs for SysID tasks.
- Explaining how the proposed INNs quantify uncertainty within their LPs.

*MATLAB implementation. [Online]. https://github.com/modifayd/INN_UQ

Algorithm 2 Training INN

```

1: Input: Training data:  $U, \hat{Y}$ 
2: Mini-batch size:  $mbs$ 
3: Number of trajectory:  $B$ 
4: Number of epochs:  $E$ 
5: Coverage:  $\alpha$ , penalty:  $\lambda$ 
6: Pre-trained NN:  $g$  with LP  $\theta^*$ .
7: Output: LP set  $\tilde{\Delta}$ 
8: Initialize  $\tilde{\Delta}$  ▷ Eq.(40)-(41)
9: for  $e = 1$  to  $E$  do
10:   for each  $mbs$  in  $B$  do
11:     Select mini-batch  $U(1:mbs, 1:N), Y(1:mbs, 1:N)$ 
12:     Construct  $X(1:mbs, 1:N)$  ▷ Eq.(8)
13:     Compute  $Y \leftarrow g(X(1:mbs, 1:N); \theta^*)$  ▷ Sec. 10
14:     Perform tricks and compute  $\underline{\Delta}_i, \bar{\Delta}_i$  ▷ Eq.(39)
15:     Define  $\tilde{\theta}$  ▷ Eq.(21)
16:     Compute  $\tilde{Y} \leftarrow \tilde{g}(X(1:mbs, 1:N); \tilde{\theta})$  ▷ Sec. IV-A
17:     Compute loss:  $L_{\text{RQR}-W}$  ▷ Eq.(35)
18:     Compute gradients:  $\partial L / \partial \tilde{\Delta}$ 
19:     Update  $\tilde{\Delta}$  via Adam optimizer
20:   end for
21: end for
22:  $\tilde{\Delta}^* = \arg \min(L_{\text{RQR}-W})$ 
23: return  $\tilde{\Delta} = \tilde{\Delta}^*$ 

```

A. Coverage Performance Analysis

We first train the LSTM and NODE models as outlined in Section III, with configurations summarized in Table I. The mean testing performance, evaluated using the Root Mean Square Error (RMSE), is shown in Table II. The comparable performance across all datasets for each model enables an effective comparison within the INNs.

ILSTM and INODE models are constructed as described in Section IV-B and IV-C, respectively. We train the following INNs, each employing a different function within the parameterization tricks defined in (39):

- ILSTM-1: ILSTM trained with σ^{ReLU} .
- ILSTM-2: ILSTM trained with σ^{abs} .
- INODE-1: ILSTM trained with σ^{ReLU} .
- INODE-2: ILSTM trained with σ^{abs} .

We trained all models using Algorithm-2 with configurations

TABLE I
DATASET CONFIGURATIONS AND HYPERPARAMETERS

		MR-Damper	Heat Exchanger	Hair Dryer
Config.	# Samples	3499	4000	1000
	Train-Val-Test Normalization	54 - 13 - 33	20 - 5 - 75	40 - 10 - 50
	N	z-score 40	min-max 80	z-score 30
(I) NODE	$n_x - n_d - n_y$	2 - 0 - 1	0 - 0 - 3	2 - 2 - 3
	# Layers	2	3	3
	Hidden Layer Size	32	35, 10	40, 40
	$r_{\text{out}} - r_{\text{hidden}}$	0.75 - 0.75	1 - 1	1 - 1
(II) LSTM	$n_x - n_d - n_y$	2 - 0 - 1	2 - 0 - 1	2 - 2 - 3
	# Layers	3	3	3
	Hidden Layer Size	48, 48	48, 48	35, 35
	$r_o - r_h$	1 - 0.2	1 - 0.2	1 - 0.2

TABLE II
TESTING RMSE PERFORMANCE COMPARISON

Dataset	LSTM	NODE
Heat Exchanger	0.556(± 0.055)	0.586(± 0.022)
MR-Damper	5.883(± 0.192)	6.659(± 0.044)
Hair Dryer	0.100(± 0.008)	0.093(± 0.006)

and hyperparameters provided in Table I. The Δ terms associated with recurrent weight U in both ILSTM-1 and ILSTM-2 were set to zero (i.e., no gradient flow) for MR Damper dataset.

We evaluated the UQ performances of the INNs by calculating the PI Coverage Probability (PICP) and PI Normalized Averaged Width (PINAW) metrics [28]. We anticipate learning an INN that attains PICP close to the desired coverage with a low PINAW value.

Table III presents the PICP and PINAW values, expressed as mean \pm standard deviation, for the desired coverage targets for these models are 90% and 95%. Fig. 1-3 present the box plots for each experiment. Here, the PICP values of box charts are generated by subtracting the calculated PICP from the target coverage. A dashed line in the middle indicates the coverage targets: 90% coverage is represented before the dashed line, while 95% coverage is shown after it. From the comparative results, we observe that:

- INODE-2 and ILSTM-2 show the best performance in terms of PICP.
- The use of the absolute function instead of ReLU provides better target coverage.
- When comparing ILSTM and INODE, the whiskers for PICP and PINAW are narrower for INODE, showing more consistent performance.

In conclusion, INODE-2 shows the best UQ performance, balancing superior coverage with slightly wider intervals compared to ILSTM-2.

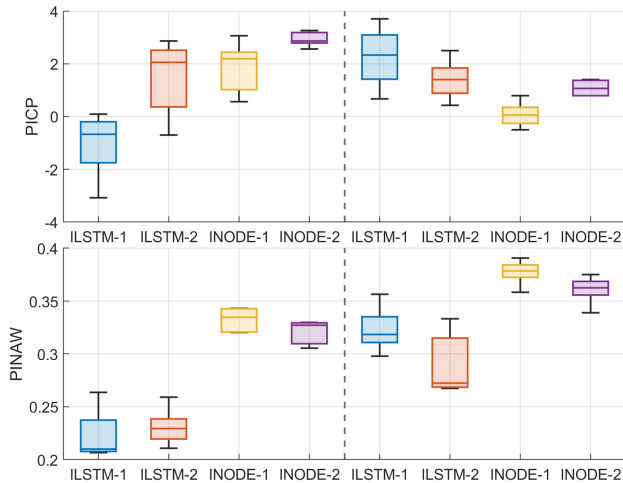


Fig. 1. Heat Exchanger Dataset: UQ Performance Comparison

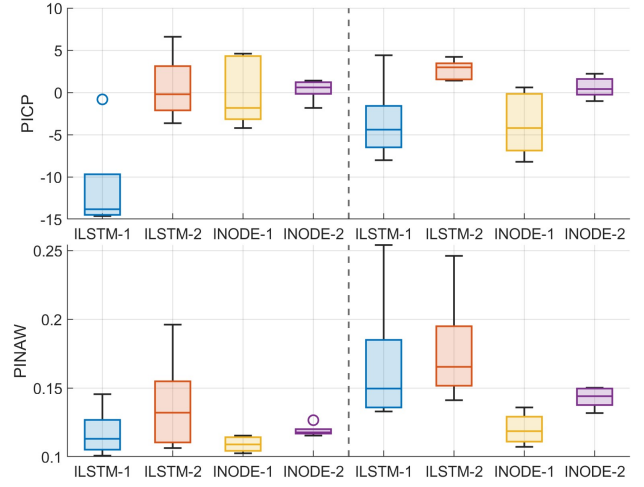


Fig. 2. Hair Dryer Dataset: UQ Performance Comparison

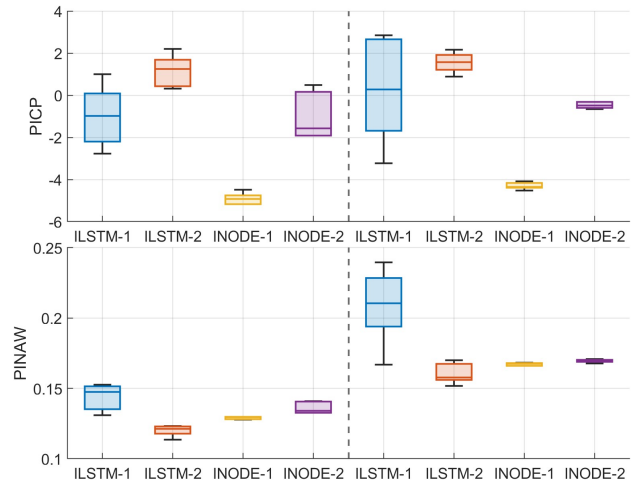


Fig. 3. MR-Damper Dataset: UQ Performance Comparison

B. Analyzing the Uncertainty Representation

This section analyzes how uncertainty is represented within the interval LPs $\hat{\theta}$ in the INN models, INODE-1 and INODE-2. The term "elasticity" is introduced to quantify the level of uncertainty in an INN parameter, defined as follows:

$$\bar{r} = \frac{\|\hat{\theta} - \theta\|}{\|\theta^*\|} \quad (42)$$

If \bar{r} is close to 0, the uncertainty in the LP is minimal, indicating that the corresponding weight or bias is well-defined and does not contribute to uncertainty. On the other hand, if \bar{r} is bigger than 1, the uncertainty is maximal, indicating that the parameter is highly uncertain. Fig. 4 illustrates the resulting \bar{r} for each weight and bias, represented as a heatmap for the given model. We can observe that:

- For INODE-2, we can observe from Fig. 4(b) that the elasticity of the weight corresponding to input 2 which is $y(k-2)$ in layer 1 introduces uncertainty for output 22. In layer 2, the elasticity of the parameters corresponding to

TABLE III
TESTING PERFORMANCE METRICS OF ILSTM AND INODE

Dataset	Metric	ILSTM-1		ILSTM-2		INODE-1		INODE-2	
		90%	95%	90%	95%	90%	95%	90%	95%
Heat Exchanger	PICP	88.95(± 1.11)	97.25(± 1.04)	91.47(± 1.30)	96.40(± 0.68)	91.84(± 0.88)	95.08(± 0.43)	92.94(± 0.25)	96.09(± 0.26)
	PINAW	22.34(± 2.16)	32.33(± 1.92)	23.07(± 1.59)	29.02(± 2.64)	33.23(± 1.00)	37.74(± 1.06)	32.72(± 1.02)	36.25(± 1.20)
MR-Damper	PICP	89.01(± 1.33)	95.27(± 2.30)	91.15(± 0.69)	96.55(± 0.44)	85.08(± 0.25)	90.70(± 0.15)	89.02(± 1.03)	94.53(± 0.14)
	PINAW	14.76(± 0.85)	21.05(± 2.45)	12.00(± 0.35)	16.07(± 0.67)	12.89(± 0.08)	16.72(± 0.09)	13.61(± 0.38)	16.95(± 0.11)
Hair Dryer	PICP	78.72(± 5.28)	91.46(± 4.24)	90.62(± 3.50)	97.68(± 1.05)	89.98(± 3.68)	91.26(± 3.39)	90.34(± 1.14)	95.59(± 1.11)
	PINAW	11.72(± 1.55)	16.70(± 4.46)	13.73(± 3.20)	17.70(± 3.65)	10.90(± 0.49)	12.01(± 1.02)	11.89(± 0.39)	14.29(± 0.68)

*PINAW values are scaled by 100.

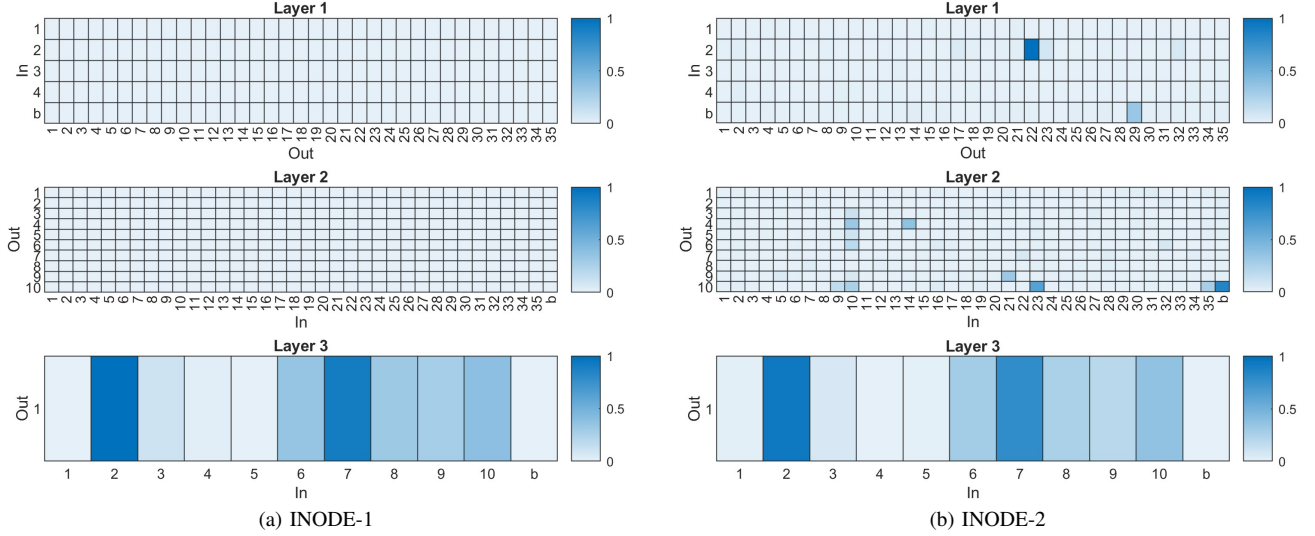


Fig. 4. Heatmaps of INN LPs from a SysID experiment on the Exchanger Dataset: (a) INODE-1 and (b) INODE-2

output 10 shows similar uncertainty. For the last layer, the elasticity is most pronounced in the parameters associated with outputs 2 and 7 of layer 2.

- For INODE-1, the elasticity of the parameters in the last layer shows significant uncertainty as shown in Fig. 4(a). The parameters associated with outputs 2 and 7 of layer 2 exhibit the highest elasticity, similar to the INODE-2.

Examining the elasticity of the parameters reveals which parts of the designed NN have a greater influence on the uncertainty of the output prediction. We observed that the parameters associated with the input $y(k-2)$ exhibit the highest levels of uncertainty. It is also observed that INODE-1 introduces uncertainty mainly in the last layer.

VII. CONCLUSION AND FUTURE WORK

This paper presents a systematic approach for constructing INNs with the capability to perform UQ for SysID tasks. The widely used NODE and LSTM networks in SysID are extended to their interval counterparts, INODE and ILSTM. A DL framework is also developed for SysID tasks, integrating a UQ loss function and parameterization tricks to ensure robust and reliable performance. Experiments with four different configurations of INODE and ILSTM reveal

that the proposed INNs successfully achieve target coverage with compact intervals. Among the configurations, INODE-2 demonstrates the best UQ performance, offering superior coverage while maintaining acceptable PI widths. Further analysis of the underlying dynamics of INODE-2, using \bar{r} values, have revealed that the θ^* corresponding to the $y(k-2)$ input resulted in the highest uncertainty. This observation highlights the model's sensitivity to the lagged output, offering valuable insights into the uncertainty contributions of specific parameters within the system.

In future research, we plan to extend the INN design to other NNs, such as CNNs, and explore their application to real-time tasks. Additionally, we aim to explore advancements in the interpretability of UQ for SysID tasks.

ACKNOWLEDGMENT

The authors acknowledge using ChatGPT to refine the grammar and enhance the English language expressions.

REFERENCES

- [1] L. Ljung, *System Identification: Theory for the User*. Prentice Hall PTR, 1999.

- [2] A. Dankers, P. M. J. Van den Hof, X. Bombois, and P. S. C. Heuberger, "Identification of dynamic models in complex networks with prediction error methods: Predictor input selection," *IEEE Transactions on Automatic Control*, vol. 61, no. 4, pp. 937–952, 2016.
- [3] N. Zhou, J. Pierre, and J. Hauer, "Initial results in power system identification from injected probing signals using a subspace method," *IEEE Transactions on Power Systems*, vol. 21, no. 3, pp. 1296–1302, 2006.
- [4] G. Pillonetto, A. Aravkin, D. Gedon, L. Ljung, A. H. Ribeiro, and T. B. Schön, "Deep networks for system identification: A survey," *Automatica*, vol. 171, p. 111907, 2025.
- [5] E. Keçeci, M. Güzelkaya, and T. Kumbasar, "A novel federated learning framework for system identification," in *2024 8th International Artificial Intelligence and Data Processing Symposium (IDAP)*. IEEE, 2024, pp. 1–6.
- [6] S. Hochreiter and J. Schmidhuber, "Long short-term memory," *Neural Comput.*, vol. 9, no. 8, p. 1735–1780, 1997.
- [7] R. T. Chen, Y. Rubanova, J. Bettencourt, and D. K. Duvenaud, "Neural ordinary differential equations," *Advances in neural information processing systems*, vol. 31, 2018.
- [8] T. Tuna, A. Beke, and T. Kumbasar, "Deep learning frameworks to learn prediction and simulation focused control system models," *Applied Intelligence*, vol. 52, no. 1, pp. 662–679, 2022.
- [9] A. Rahman, J. Dragoña, A. Tuor, and J. Strube, "Neural ordinary differential equations for nonlinear system identification," in *American Control Conference*, 2022, pp. 3979–3984.
- [10] C. Coelho, M. F. P. Costa, and L. L. Ferrás, "Enhancing continuous time series modelling with a latent ode- lstm approach," *Applied Mathematics and Computation*, vol. 475, p. 128727, 2024.
- [11] C. J. Roy and W. L. Oberkampf, "A comprehensive framework for verification, validation, and uncertainty quantification in scientific computing," *Computer methods in applied mechanics and engineering*, vol. 200, no. 25–28, pp. 2131–2144, 2011.
- [12] M. Abdar, F. Pourpanah, S. Hussain, D. Rezazadegan, L. Liu, M. Ghavamzadeh, P. Fieguth, X. Cao, A. Khosravi, U. R. Acharya *et al.*, "A review of uncertainty quantification in deep learning: Techniques, applications and challenges," *Information fusion*, vol. 76, pp. 243–297, 2021.
- [13] Y. Güven, A. Köklü, and T. Kumbasar, "Exploring zadeh's general type-2 fuzzy logic systems for uncertainty quantification," *IEEE Transactions on Fuzzy Systems*, 2024.
- [14] A. Köklü, Y. Güven, and T. Kumbasar, "Odyssey of interval type-2 fuzzy logic systems: Learning strategies for uncertainty quantification," *IEEE Transactions on Fuzzy Systems*, 2024.
- [15] T. Pearce, A. Brintrup, M. Zaki, and A. Neely, "High-quality prediction intervals for deep learning: A distribution-free, ensembled approach," in *Proceedings of the International Conference on Machine Learning*, vol. 80, 2018, pp. 4075–4084.
- [16] A. Khosravi, S. Nahavandi, D. Creighton, and A. F. Atiya, "Comprehensive review of neural network-based prediction intervals and new advances," *IEEE Transactions on Neural Networks*, vol. 22, no. 9, pp. 1341–1356, 2011.
- [17] M. Morimoto, K. Fukami, R. Maulik, R. Vinuesa, and K. Fukagata, "Assessments of epistemic uncertainty using gaussian stochastic weight averaging for fluid-flow regression," *Physica D: Nonlinear Phenomena*, vol. 440, p. 133454, 2022.
- [18] M. R. Baker and R. B. Patil, "Universal approximation theorem for interval neural networks," *Reliable Computing*, vol. 4, pp. 235–239, 1998.
- [19] Y. Mao, M. N. Müller, M. Fischer, and M. Vechev, "Understanding certified training with interval bound propagation," *arXiv preprint arXiv:2306.10426*, 2023.
- [20] K. Tretiak, G. Schollmeyer, and S. Ferson, "Neural network model for imprecise regression with interval dependent variables," *Neural Networks*, vol. 161, pp. 550–564, 2023.
- [21] J. Sadeghi, M. de Angelis, and E. Patelli, "Efficient training of interval neural networks for imprecise training data," *Neural Networks*, vol. 118, pp. 338–351, 2019.
- [22] L. Oala, C. Heiß, J. Macdonald, M. März, W. Samek, and G. Kutylniok, "Interval neural networks: Uncertainty scores," *arXiv preprint arXiv:2003.11566*, 2020.
- [23] T. Hickey, Q. Ju, and M. H. Van Emden, "Interval arithmetic: From principles to implementation," *J. ACM*, vol. 48, no. 5, p. 1038–1068, 2001.
- [24] T. Zhang, Z. Yao, A. Gholami, J. E. Gonzalez, K. Keutzer, M. W. Mahoney, and G. Biro, "Anodev2: A coupled neural ode framework," *Advances in Neural Information Processing Systems*, vol. 32, 2019.
- [25] T. Pouplin, A. Jeffares, N. Seedat, and M. van der Schaar, "Relaxed quantile regression: Prediction intervals for asymmetric noise," *arXiv preprint arXiv:2406.03258*, 2024.
- [26] J. Wang, A. Sano, T. Chen, and B. Huang, "Identification of hammerstein systems without explicit parameterisation of non-linearity," *International Journal of Control*, vol. 82, no. 5, pp. 937–952, 2009.
- [27] B. De Moor, R. D. Bie, I. Lemahieu, and J. Renders, "Daisy: Database for the identification of systems," <http://homes.esat.kuleuven.be/~smc/daisy/>, 1997, accessed 13 Jan 2025.
- [28] H. Quan, D. Srinivasan, and A. Khosravi, "Short-term load and wind power forecasting using neural network-based prediction intervals," *IEEE Transactions on Neural Networks and Learning Systems*, vol. 25, no. 2, pp. 303–315, 2014.